PROCEEDINGS OF SCIENCE

Inclusive radiative electroweak penguin decays: $b \to s\gamma$

Luis Pesántez[*†]
University of Melbourne
E-mail: luis.pesantez@coepp.org.au

The inclusive radiative decay $b \to s\gamma$ is a flavor-changing-neutral-current that proceeds through an electroweak penguin loop. The observables related to the decay can be precisely calculated in the Standard Model up to next-to-next-to-leading order and have been measured to a few percent accuracy. For these reasons they can provide with strong constraints on supersymmetric models and other New Physics models that predict additional Higgs scalars, or other new particles exchanged in the penguin loop. The B-factories have performed measurements of the *BF*s and CP-asymmetries using different experimental approaches: inclusive and sum of exclusive final states. We present the latest results from Belle and BABAR, give prospects for the precision expected at Belle II and present updated limits on type II Two Higgs Doublet Model parameters.

Flavor Physics & CP Violation 2015,
May 25-29, 2015
Nagoya, Japan

[*]Speaker.
[†]On behalf of the Belle Collaboration.

1. Introduction

The decays $b \to d\gamma$ and $b \to s\gamma$ are flavor-changing neutral currents (FCNC), forbidden at tree level in the Standard Model (SM). They proceed via electroweak penguin diagrams, where a top quark and a charged weak boson are exchanged. The transitions are sensitive to potential contributions of heavy charged non-SM particles. In the operator product expansion (OPE) [1], the effective Hamiltonian that governs weak decays can be expressed as the sum of operators $\mathscr{O}_i$ with corresponding Wilson coefficients C_i: $H_{\text{eff}} = \frac{G_F}{\sqrt{2}} \sum_i V^i_{\text{CKM}} C_i(\mu) O_i$. For the decays $b \to d\gamma$ and $b \to s\gamma$, the O_7 and O_8 operators, and C_7 and C_8 coefficients [2], contain all physical information. Since new particles would modify observables such as the branching fraction (BF) or CP-asymmetry ($\mathscr{A}_{CP}$), this can be expressed as modifications to the relevant Wilson coefficients.

The SM gives precise predictions for the inclusive decays. The most recent calculation of the $b \to s\gamma$ BF is complete up to NNLO and has a 7 % total uncertainty [3]. This calculation is consistent with the 2014 world average [4], which also has a 7 % precision:

$$\mathscr{B}(b \to s\gamma)_{\text{SM}} = (3.36 \pm 0.23) \times 10^{-4} \tag{1.1}$$

$$\mathscr{B}(b \to s\gamma)_{\text{exp}} = (3.43 \pm 0.21\ (\text{stat}) \pm 0.07\ (\text{syst})) \times 10^{-4} \tag{1.2}$$

Such precise theoretical predictions motivate inclusive and semi-inclusive analyses, for which various experimental approaches exist. Theoretical calculations are based on a photon energy threshold of 1.6 GeV, this poses a challenge for a measurement since the amount of background increases drastically when going to such low energies. Measurements of the BF are typically performed for energies above 1.9 GeV and extrapolated to the lower threshold.

CP-asymmetries are important observables that can be constructed in two ways for this decays: flavor tagged and untagged. This means one can measure $\mathscr{A}_{CP}$ for the $b \to s\gamma$ or $b \to d\gamma$ decays ($\mathscr{A}_{CP}$ $(b \to s\gamma)$ and $\mathscr{A}_{CP}$ $(b \to d\gamma)$), or for both inclusively $\mathscr{A}_{CP}$ $(b \to s/d\gamma)$. The standard model predicts non-vanishing asymmetries in the tagged cases [5], but also an almost perfect cancellation of CP-violating effects in the untagged case [6], that leads to vanishing theoretical uncertainties. If new-physics (NP) effects appear, they will affect both tagged and untagged asymmetries which would show a strong proportionality, therefore a measurement of both quantities is necessary [6].

Two-Higgs-Double models (2HDM) [7] are a popular NP-model choice. Here, the SM Lagrangian is modified by the inclusion of an additional Higgs doublet, this translates in a theory with a total of three neutral and two charged Higgs scalars. The most widely studied is the type II (2HDM-II), it does not allow for tree level FCNC and its flavor structure resembles that of the minimal supersymmetric model. Flavor measurements can do a very good job constraining the parameter space of 2HDM-II. The two parameters of relevance are the mass of the charged Higgs scalar ($M(H^+)$) and the ratio of vevs for the two scalars ($\tan\beta$). The $b \to s\gamma$ BF allows to set a bound on $M(H^+)$ of > 480 GeV, according to the latest theoretical calculation [3].

2. Experimental considerations

As noted before, the best test of the SM in this decay comes from inclusive analyses. They rely on the reconstruction of either a single high energy photon, several different final states, or the

full reconstruction of a tag-side B meson, therefore they can only be performed in the environment of a B-factory. Belle and BABAR have recorded large samples at the $\Upsilon(4S)$ resonance, which decays to a $B\bar{B}$ pair. Both experiments have collected respectively 770×10^6 and 470×10^6 $B\bar{B}$ pairs, allowing the achievement of high precision in these measurements. The data samples used to study continuum background ($e^+e^- \to q\bar{q}$) must be also considered. They are taken at an energy below the $\Upsilon(4S)$, and are much smaller in size, with respect to the $\Upsilon(4S)$ samples (about 10 times smaller). Continuum is one of the most important backgrounds when performing fully inclusive analyses, therefore a small sample size has an impact on the achievable statistical precision.

3. Experimental approaches

3.1 Semi-inclusive method

In the semi-inclusive approach (sum of exclusive final states), as many exclusive final states as possible are reconstructed in order to reduce the uncertainty from unmeasured modes. The B meson is reconstructed as the combination of a photon with energy > 1.9 GeV in the center of mass frame (CM), and one of 38 hadronic X_s final states. The X_s states consist of up to three kaons (K^+, K^0_S) with at most one K^0_S, up to four pions (π^+, π^0) with at most two π^0 and at most one η meson [8, 9]. The suppression of continuum background is performed through multivariate classifiers that exploit topological differences between continuum and $B\bar{B}$ events. They are optimized for different hadronic mass bins in such a way that they provide high background suppression but still keep a high signal selection efficiency.

The extraction of the signal proceeds as fit to the beam constrain mass ($M_{\rm bc}$) variable. It is defined as: $M_{\rm bc} = \sqrt{E^{*2}_{\rm beam} - p^{*2}_B}$ with p^*_B the CM momentum of the reconstructed B, it peaks around the nominal B mass for signal events. The fit to $M_{\rm bc}$ is performed in 18 (BABAR) or 19 (Belle) M_{X_s} bins. The fit has signal, cross-feed, peaking background and combinatoric background components. Examples of the fits are shown in Fig. 1, for the region $1.4\ {\rm GeV/c^2} \leq {\rm M_{X_s}} \leq 1.5\ {\rm GeV/c^2}$ for the Belle and BABAR analyses.

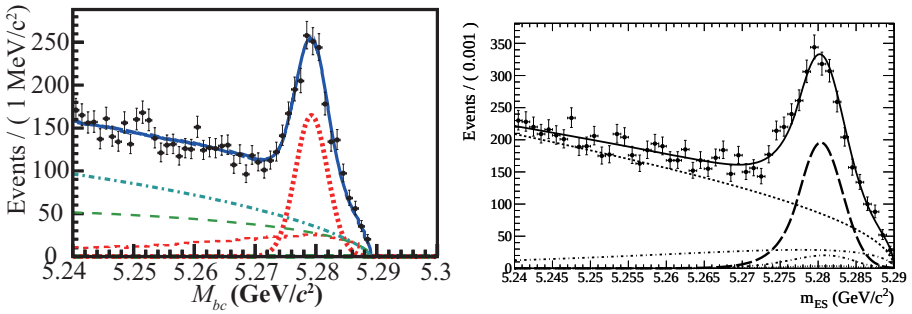

Figure 1: Result of the fit to $M_{\rm bc}$ in the bin $1.4\ {\rm GeV/c^2} \leq {\rm M_{X_s}} \leq 1.5\ {\rm GeV/c^2}$ for the Belle (left) and BABAR (right) analyses [8, 9]. The Belle fit components are: signal (solid red), crossfeed (dashed red), peaking background (solid green), non-peaking $B\bar{B}$ background (dashed green) and continuum (dot-dashed cyan). The BABAR components are: signal (thick dashed), cross-feed (two dot-dashed), peaking $B\bar{B}$ (dotted), and combinatoric background (thin dashed).

An important step is the determination of the selection efficiencies for the individual modes, this is done by tuning the JETSET parameters, which is used to model the X_s fragmentation, such that it reproduces the data efficiency properly. The dominant systematic uncertainties arise from non reconstructed final states (between 1% and 30%, depending on the M_{X_s} bin), the fitting PDFs ($\sim 4\%$) and the detector response ($\sim 3\%$). In Fig. 2 the partial BF in M_{X_s} bins is shown, the total BFs for a 1.9 GeV threshold are quoted below:

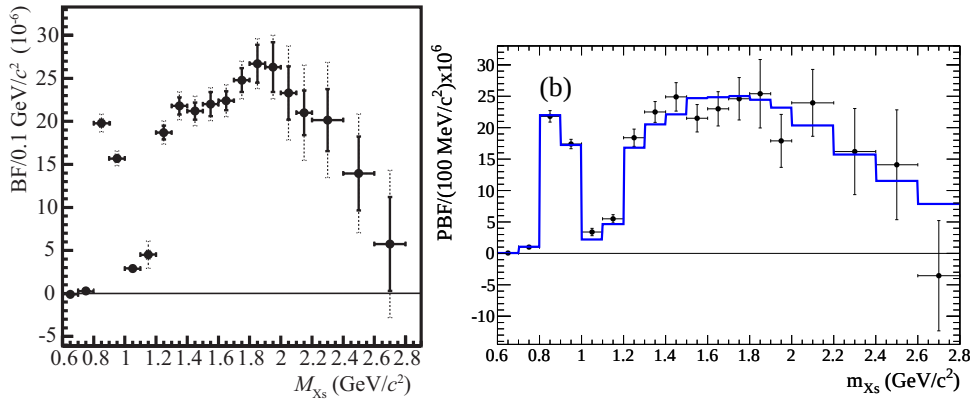

Figure 2: Partial BFs for the Belle (left) and BABAR (right) semi-inclusive analyses [8, 9].

$$\text{Belle} \quad \mathscr{B}(B \to X_s\gamma) = (3.51 \pm 0.17 \pm 0.33) \times 10^{-4}$$
$$\text{BABAR} \quad \mathscr{B}(B \to X_s\gamma) = (3.29 \pm 0.19 \pm 0.48) \times 10^{-4}$$

Using 16 of the reconstructed final states, BABAR has measured the direct CP asymmetry and the CP asymmetry difference between charged and neutral modes [10]. The observables are defined as:

$$\mathscr{A}_{CP}(b \to s\gamma) = \frac{\Gamma(\bar{B} \to \bar{X}_s\gamma) - \Gamma(B \to X_s\gamma)}{\Gamma(\bar{B} \to \bar{X}_s\gamma) + \Gamma(B \to X_s\gamma)} \tag{3.1}$$

$$\Delta\mathscr{A}_{CP} = B^+ \to X_s\gamma - B^0 \to X_s\gamma \tag{3.2}$$

The direct CP asymmetry is predicted to be in the range $-0.6\% < \mathscr{A}_{CP}(B \to X_s\gamma)_{\text{SM}} < 2.8\%$ [5]. The CP asymmetry difference is proportional to the imaginary part of the C_7 and C_8 Wilson coefficients: $\Delta\mathscr{A}_{CP} \approx 4\pi^2\alpha_s \frac{\bar{\Lambda_7 8}}{m_b} \Im\left(\frac{C_8}{C_7}\right)$.

The measured value is $\mathscr{A}_{CP}B \to X_s\gamma = (1.7 \pm 1.9 \pm 1.0)\%$, consistent with SM expectations. Additionally from the measured value for the difference $\Delta\mathscr{A}_{CP} = (5.0 \pm 3.9 \pm 1.5)\%$, confidence intervals for the ratio $\Im\left(\frac{C_8}{C_7}\right)$ can be derived and are shown in Fig. 3.

3.2 Inclusive measurement

In the inclusive analysis only the photon from the radiative decay is selected. Photons with CM energy 1.7 GeV $-$ 2.8 GeV are considered. Additionally a charged lepton from the tag B meson is reconstructed for two purposes: background suppression and flavor tagging. The charge of the

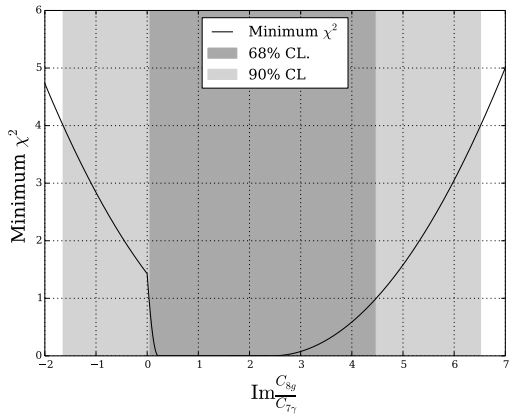

Figure 3: Confidence intervals for the ratio $\Im\left(\frac{C_8}{C_7}\right)$ [10].

lepton determines uniquely the flavor of the B mesons. There is a large number of background photons arising from the decays $\pi^0(\eta) \to \gamma\gamma$, they are vetoed. Continuum background is suppressed with the use of multivariate discriminants [11, 12, 13].

The BABAR analysis uses a 1.9 GeV threshold, the main systematics in the measurement of the BF come from the modelling of $B\bar{B}$ background (7.8%), and the uncertainty on the selection efficiency (3.1%) [12]. The Belle analysis uses a 1.7 GeV threshold and has dominant systematic uncertainties from continuum and $B\bar{B}$ background estimation (7.5% each). The photon energy spectrum for both analyses is shown in Fig. 4. The analyses measure:

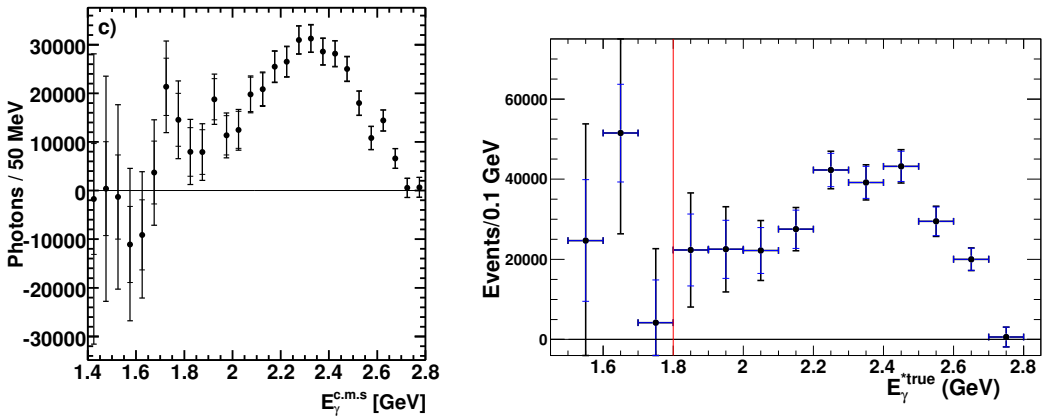

Figure 4: Photon energy spectrum for the Belle (left) and BABAR (right) inclusive analyses [11, 12].

$$\begin{aligned}
\text{BABAR}: \quad & \mathscr{B}(B \to X_s\gamma) = (3.00 \pm 0.14 \pm 0.19 \pm 0.06) \times 10^{-4} \ (\mathrm{E}^*_\gamma > 1.9 \text{ GeV}) \\
\text{Belle}: \quad & \mathscr{B}(B \to X_s\gamma) = (3.45 \pm 0.15 \pm 0.40) \times 10^{-4} \ (\mathrm{E}^*_\gamma > 1.7 \text{ GeV}) \\
\text{Belle}: \quad & \mathscr{B}(B \to X_s\gamma) = (3.21 \pm 0.11 \pm 0.16) \times 10^{-4} \ (\mathrm{E}^*_\gamma > 1.9 \text{ GeV})
\end{aligned}$$

The untagged CP-asymmetry, $\mathscr{A}_{CP}$ $(B \to X_{s+d}\gamma)$, can be measured using the charge of the reconstructed lepton to tag the B flavor. A dilution factor ω arises since in some cases the reconstructed lepton charge does not correspond to the actual signal B flavor. The measured and true asymmetries are related as: $\mathscr{A}_{CP}^{\text{true}} = \frac{1}{1-2\omega}\mathscr{A}_{CP}^{\text{meas}}$. The effects contributing to this factor are: oscillation of neutral B mesons, secondary leptons and hadrons misreconstructed as leptons. The systematic uncertainties for this measurement arise mainly from the determination of possible charge asymmetries in the reconstruction of leptons or a charge asymmetry induced by the detection of charged tracks. They are in any case small and the measurement is limited by the statistical precision. For $E^*_\gamma > 2.1$ GeV BABAR and Belle measure:

$$\begin{aligned}
\text{BABAR}: \quad & \mathscr{A}_{CP}(B \to X_{s+d}\gamma) = (5.7 \pm 6.0 \pm 1.8) \times 10^{-2} \\
\text{Belle}: \quad & \mathscr{A}_{CP}(B \to X_{s+d}\gamma) = (2.2 \pm 3.9 \pm 0.9) \times 10^{-2}
\end{aligned}$$

4. New limits on Two-Higgs-Double Model of type II

Flavor processes can receive contributions of charged Higgs scalars, as the one predicted by the 2HDM-II. The charged Higgs could be present as a mediator in Feynman diagrams were typically only a charged weak boson is present. The ratio $R(B \to X_s\gamma) = \frac{\mathscr{B}(B\to X_s\gamma)}{\mathscr{B}(B\to X\ell\nu)}$ can be used to constrain the mass of such Higgs particle. Measurements of leptonic branching fractions (decays of the form $M \to \ell\nu$) can constrain the parameter space in the ratio $\tan\beta/M(H^+)$. Other observables such as the B^0 or B^0_s oscillation frequencies ($\Delta m_{d,s}$), can rule out a low values of $\tan\beta$.

Making use of the CKMfitter framework, we are able to combine several different flavor measurements and obtain limits for the 2HDM-II in the $\tan\beta - M(H^+)$ parameter space [14]. The limits are plotted on Fig. 5, here we also show limits from direct searches by LEP [15] and ATLAS [16]. It is worth noting that the 95% CL allowed regions are coloured. For the calculation we have used the latest measurements of the following quantities: $\frac{K\to\ell\nu}{\pi\to\ell\nu}$, $\frac{\tau\to K\nu}{\tau\to\pi\nu}$, $\frac{K\to\pi\mu\nu}{K\to\pi e\nu}$, $\mathscr{B}(Ds \to \mu\nu)$, $\mathscr{B}(D \to \mu\nu)$, $\mathscr{B}(B \to \tau\nu)$ $R_b = \frac{Z\to b\bar{b}}{Z\to\text{hadrons}}$ and the $B_{s,d}\bar{B}_{s,d}$ oscillation frequencies. The average of the $B \to X_s\gamma$ BF is obtained using the inclusive and semi-inclusive measurements by BABAR and Belle and extrapolating them to 1.6 GeV, this new average is $\mathscr{B}(B \to X_s\gamma)_{\text{avg}} = (3.41 \pm 0.16(\text{exp}) \pm 0.04(\text{extrap})) \times 10^{-4}$, and puts the lower limit on $M(H^+) \gtrsim 540$ GeV at 95% CL. The leptonic decays allow for NP in the parameter space region $\tan\beta/M(H^+) \lesssim 0.85$, whereas loop and box processes allow for $\tan\beta \gtrsim 1$.

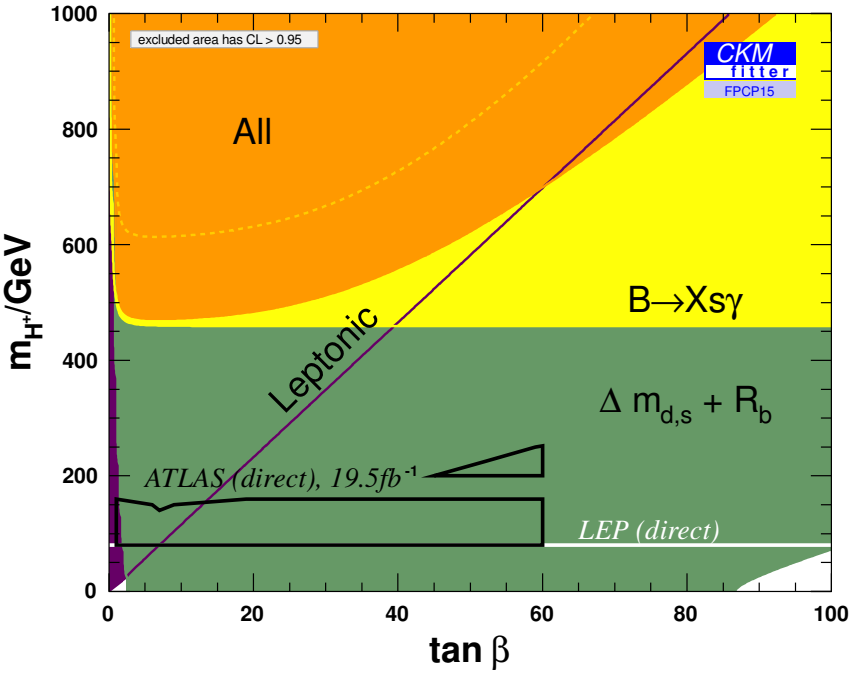

Figure 5: Limits on the $\tan\beta - M(H^+)$ parameter space of the 2HDM-II. The coloured regions are allowed with a 95% CL. The orange region is the combination of $B \to X_s\gamma$, leptonic and loop measurements. The dashed yellow region delimits the allowed 68% CL region.

5. Conclusion and outlook

The transitions $b \to d\gamma$ and $b \to s\gamma$ provide a rich set of observables that can be used to test the SM. The statistical precision is the limiting factor in some of the presented measurements. A better understanding of the X_s hadronization would greatly improve the precision on the branching fraction measurement in the semi-inclusive approach. When considering these effects, it can be concluded that there is plenty of room for improvement when the large data sets from Belle II become available. Additional to these well established experimental techniques, the analysis of $B \to X_s\gamma$ using a full hadronic tag [17] will become feasible due to the large statistics compete with the traditional techniques. When projecting the current experimental precision for the different approaches, one can observe that for a full Belle II data set, all are very competitive, Fig. 6. This paints an exciting panorama for the future of $b \to s\gamma$.

References

[1] A. J. Buras, Lect. Notes Phys. **558**, 65 (2000) [hep-ph/9901409].

[2] T. Hurth, E. Lunghi and W. Porod, Nucl. Phys. B **704** (2005) 56 [hep-ph/0312260].

[3] M. Czakon, P. Fiedler, T. Huber, M. Misiak, T. Schutzmeier and M. Steinhauser, JHEP **1504**, 168 (2015) [arXiv:1503.01791 [hep-ph]].

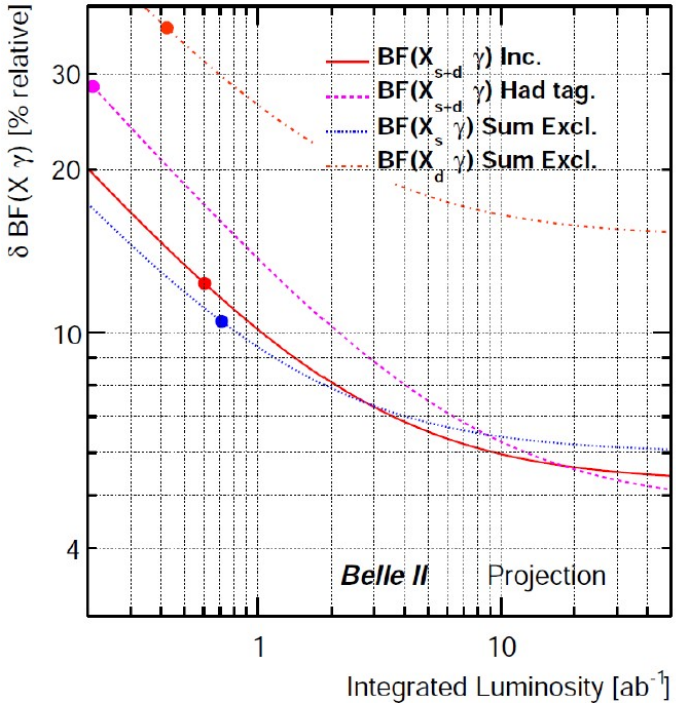

Figure 6: Expected precision of the measurements on the $B \to X_s\gamma$ branching fraction for different experimental approaches.

[4] Y. Amhis *et al.* [Heavy Flavor Averaging Group (HFAG) Collaboration],

[5] M. Benzke, S. J. Lee, M. Neubert and G. Paz, Phys. Rev. Lett. **106**, 141801 (2011), [arXiv:1012.3167 [hep-ph]].

[6] T. Hurth, E. Lunghi and W. Porod, Nucl. Phys. B **704**, 56 (2005), [hep-ph/0312260].

[7] G. C. Branco, P. M. Ferreira, L. Lavoura, M. N. Rebelo, M. Sher and J. P. Silva, Phys. Rept. **516**, 1 (2012) [arXiv:1106.0034 [hep-ph]].

[8] T. Saito *et al.* [Belle Collaboration], Phys. Rev. D **91**, no. 5, 052004 (2015) [arXiv:1411.7198 [hep-ex]].

[9] J. P. Lees *et al.* [BaBar Collaboration], Phys. Rev. D **86**, 052012 (2012) [arXiv:1207.2520 [hep-ex]].

[10] J. P. Lees *et al.* [BaBar Collaboration], Phys. Rev. D **90**, no. 9, 092001 (2014) [arXiv:1406.0534 [hep-ex]].

[11] A. Limosani *et al.* [Belle Collaboration], Phys. Rev. Lett. **103**, 241801 (2009) [arXiv:0907.1384 [hep-ex]].

[12] J. P. Lees *et al.* [BaBar Collaboration], Phys. Rev. D **86**, 112008 (2012) [arXiv:1207.5772 [hep-ex]].

[13] L. Pesántez *et al.* [Belle Collaboration], Phys. Rev. Lett. **114**, no. 15, 151601 (2015) [arXiv:1501.01702 [hep-ex]].

[14] O. Deschamps, S. Descotes-Genon, S. Monteil, V. Niess, S. T'Jampens and V. Tisserand, Phys. Rev. D **82**, 073012 (2010) [arXiv:0907.5135 [hep-ph]].

[15] G. Abbiendi *et al.* [ALEPH and DELPHI and L3 and OPAL and LEP Collaborations], Eur. Phys. J. C **73**, 2463 (2013) [arXiv:1301.6065 [hep-ex]].

[16] G. Aad *et al.* [ATLAS Collaboration], JHEP **1503**, 088 (2015) [arXiv:1412.6663 [hep-ex]].

[17] B. Aubert *et al.* [BaBar Collaboration], Phys. Rev. D **77**, 051103 (2008) [arXiv:0711.4889 [hep-ex]].